Applications in Plant Sciences

Botanical Society of America
leading scientists and educators since 1893

APPLICATION ARTICLE

Virus-induced gene silencing as a tool for functional studies in *Cleome violacea*

Shane Carey[1,4,*], Mónica Higuera-Díaz[1,*], Peter Mankowski[1,2], Alexandra Rocca[1,3], and Jocelyn C. Hall[1]

Manuscript received 18 January 2021; revision accepted 5 May 2021.

[1] Department of Biological Sciences, University of Alberta, Edmonton, Alberta, Canada

[2] Current address: Department of Surgery, University of British Columbia, Vancouver, British Columbia, Canada

[3] Current address: Administration Building, University of Alberta, Edmonton, Alberta, Canada

[4] Author for correspondence: scarey@ualberta.ca

*These authors contributed equally to this work.

Citation: Carey, S., M. Higuera-Díaz, P. Mankowski, A. Rocca, and J. C. Hall. 2021. Virus-induced gene silencing as a tool for functional studies in *Cleome violacea*. *Applications in Plant Sciences* 9(5): e11435.

doi:10.1002/aps3.11435

PREMISE: Cleomaceae is emerging as a promising family to investigate a wide range of phenomena, such as C_4 photosynthesis and floral diversity. However, functional techniques are lacking for elucidating this diversity. Herein, we establish virus-induced gene silencing (VIGS) as a method of generating functional data for *Cleome violacea*, bolstering Cleomaceae as a model system.

METHODS: We leveraged the sister relationship of Cleomaceae and Brassicaceae by using constructs readily available for *Arabidopsis thaliana* to provide initial information about the feasibility of VIGS in *C. violacea*. We then developed endogenous constructs to optimize VIGS efficiency and viability for fruit development.

RESULTS: *PHYTOENE DESATURASE* was successfully downregulated in *C. violacea* using both heterologous and endogenous constructs. The endogenous construct had the highest degree of downregulation, with many plants displaying strong photobleaching. *FRUITFULL*-treated plants were also successfully downregulated, with a high rate of survival but less effective silencing; only a small percentage of survivors showed a strong phenotype.

DISCUSSION: Our optimized VIGS protocol in *C. violacea* enables functional gene analyses at different developmental stages. Additionally, *C. violacea* is amenable to heterologous knockdown, which suggests that a first pass using non-endogenous constructs is a possible route to test additional species of Cleomaceae.

KEY WORDS Cleomaceae; *Cleome violacea*; emerging model; *FRUITFULL*; *PHYTOENE DESATURASE*; virus-induced gene silencing.

Cleomaceae is a pantropical plant family comprising approximately 270 morphologically diverse species (Patchell et al., 2014), and despite having only a few economically important taxa, it is emerging as a model clade to investigate many areas of research (reviewed in Bayat et al., 2018). These topics include floral morphology and development (Nozzolillo et al., 2010; Patchell et al., 2011; Endress, 2016), pollination biology (Cane, 2008; Higuera-Díaz et al., 2015), comparative genomics/transcriptomics (Schranz and Mitchell-Olds, 2006; Barker et al., 2009; Bräutigam et al., 2011a, 2011b; Cheng et al., 2013; Bhide et al., 2014; Külahoglu et al., 2014), evolution of C_4 photosynthesis (Marshall et al., 2007; Voznesenskaya et al., 2007; Bräutigam et al., 2011a; Koteyeva et al., 2011, 2014; Williams et al., 2015), and glucosinolates (van den Bergh et al., 2016). An attractive feature of this family is its sister relationship to the Brassicaceae, which houses the model species *Arabidopsis thaliana* (L.) Heynh. This close phylogenetic distance facilitates transfer of knowledge from *A. thaliana* while permitting the investigation of morphological and physiological traits not found in Brassicaceae. These traits include substantive floral diversity and C_4 photosynthesis (Bayat et al., 2018). Furthermore, research of these traits is facilitated by steadily growing –omics data within Cleomaceae, including published genomes of *Tarenaya hassleriana* (Chodat) Iltis (Cheng et al., 2013) and *Cleome violacea* L. (https://genomevolution.org/coge; accession no. 23822), as well as transcriptomic data from flowers and leaves of *T. hassleriana* and *Gynandropsis gynandra* (L.) Briq. (Bräutigam et al., 2011a; Bhide et al., 2014; Kulahoglu et al., 2014). In summary, Cleomaceae is a promising group to investigate important ecological and evolutionary phenomena.

Reverse genetics is key to understanding the mechanisms underlying morphological diversity in Cleomaceae because it directly tests the role(s) of candidate genes generating that diversity. Stable transformation techniques have been developed for both *G. gynandra* and *Tarenaya spinosa* (Jacq.) Raf. (Newell et al., 2010; Tsai et al., 2012), but they are time-consuming, in part because they require cell culture. To the best of our knowledge,

only one study has used stable transformation in Cleomaceae to empirically examine mechanisms regulating C_4 photosynthesis in *G. gynandra* (Williams et al., 2015). An effective alternative to stable transformation is virus-induced gene silencing (VIGS), which is a well-established post-transcriptional gene silencing (PTGS) tool used in many model and non-model species (Burch-Smith et al., 2004, 2006; Gould and Kramer, 2007; Becker and Lange, 2010; Di Stilio et al., 2010; Becker, 2013). VIGS uses RNA interference to exploit plant defenses, which greatly reduces endogenous mRNA transcription without the need for stable transformation over multiple generations (Ruiz et al., 1998; Baulcombe, 1999; Burch-Smith et al., 2004). Thus, VIGS provides the opportunity to quickly downregulate individual or multiple genes and infer function via the observation of modified phenotype (Becker and Lange, 2010; Becker, 2013). Notwithstanding the potential of VIGS for examining gene function in a range of species, protocols must be tailored for each new species (Senthil-Kumar et al., 2007; Becker, 2013). Tailoring of protocols can be challenging because of factors like developmental timing, susceptibility to *Agrobacterium tumefaciens* infection, and strength of PTGS response. Furthermore, not all species are amenable to reverse genetic approaches like VIGS.

Cleome violacea is a species of note for investigations within Cleomaceae (Mabry et al., 2020) and an ideal candidate for VIGS. It has a published genome and exhibits morphological traits that are important for pollinator interactions, e.g., floral monosymmetry and prominent nectaries (Fig. 1). Furthermore, *C. violacea* displays features that facilitate its study, including small stature, high fecundity, self-fertilization, and short generation time. Here, we report on testing and optimizing the VIGS methodology in *C. violacea*. Specifically, the goals of this study are threefold: (1) establish that constructs with heterologous sequences are an informative first screen to determine efficacy of VIGS in *C. violacea*, (2) optimize the VIGS protocol for *C. violacea*, and (3) demonstrate that this protocol is effective for multiple developmental stages. We selected two genes that would maximize comparison of *C. violacea* to other VIGS models and that would adequately test different developmental processes. First, *PHYTOENE DESATURASE* (*PDS*) is commonly used to determine the efficacy of VIGS in many systems due to its easy-to-score bleaching phenotype when downregulated (Gould and Kramer, 2007; Senthil-Kumar et al., 2007; Wege et al., 2007; Velasquez et al., 2009; Fujita et al., 2019). Second, the MADS-box transcription factor *FRUITFULL* (*FUL*) has an established role in fruit development in *A. thaliana* (Gu et al., 1998; Ferrándiz et al., 2000a, 2000b; Ferrándiz and Fourquin, 2014; Eldridge et al., 2016), a species with similar fruit morphology to *C. violacea* (Fig. 2B). Furthermore, fruit development is the last stage in reproduction and, as such, successful downregulation of *FUL* would demonstrate the efficacy of VIGS across multiple developmental stages in *C. violacea*.

FIGURE 1. *Cleome violacea* whole plant (A), ventral view of flower (B), and lateral view of flower (C).

METHODS

Plant growth conditions

Inbred lines of *C. violacea* were grown from lab seed stock, and a voucher was deposited in the Vascular Plant Herbarium (ALTA) at the University of Alberta (Hall & Bolton s.n., 20 Feb 2008; #813 from *Hortus Botanicus*, Amsterdam). Seeds were sown in groups of 10 using 10-cm-wide square pots, and individual plants were transferred after treatments to 7.5-cm-diameter round pots. Growth substrate was a 2 : 1 mixture of sterilized (liquid cycle, 121.1°C, 20 min) Sun Gro Sunshine Mix (Sun Gro Horticulture, Agawam, Massachusetts, USA) and perlite. All plants were grown in a growth chamber at the Department of Biological Sciences at the University of Alberta, with 16 h of light and 8 h of darkness at 24°C. This temperature was chosen for *C. violacea* because it falls within the optimal range for VIGS silencing reported in *Arabidopsis thaliana* (22–24°C) (Wang et al., 2006) while maintaining fast and efficient plant growth. However, it is important to note that *C. violacea* grows well under a range of growth conditions (e.g., small to large pots, temperatures between 20–26°C, and growth medium without perlite).

Cloning and viral vector construct design

Viral vector construct design and inoculation were carried out in accordance with previous VIGS protocols (Gould and Kramer, 2007; Kramer et al., 2007). Tobacco rattle virus vectors pTRV1 (donor stock no. YL192), pTRV2 (donor stock no. YL156), and pTRV2-*AtPDS* (donor stock no. YL154) were obtained from The Arabidopsis Information

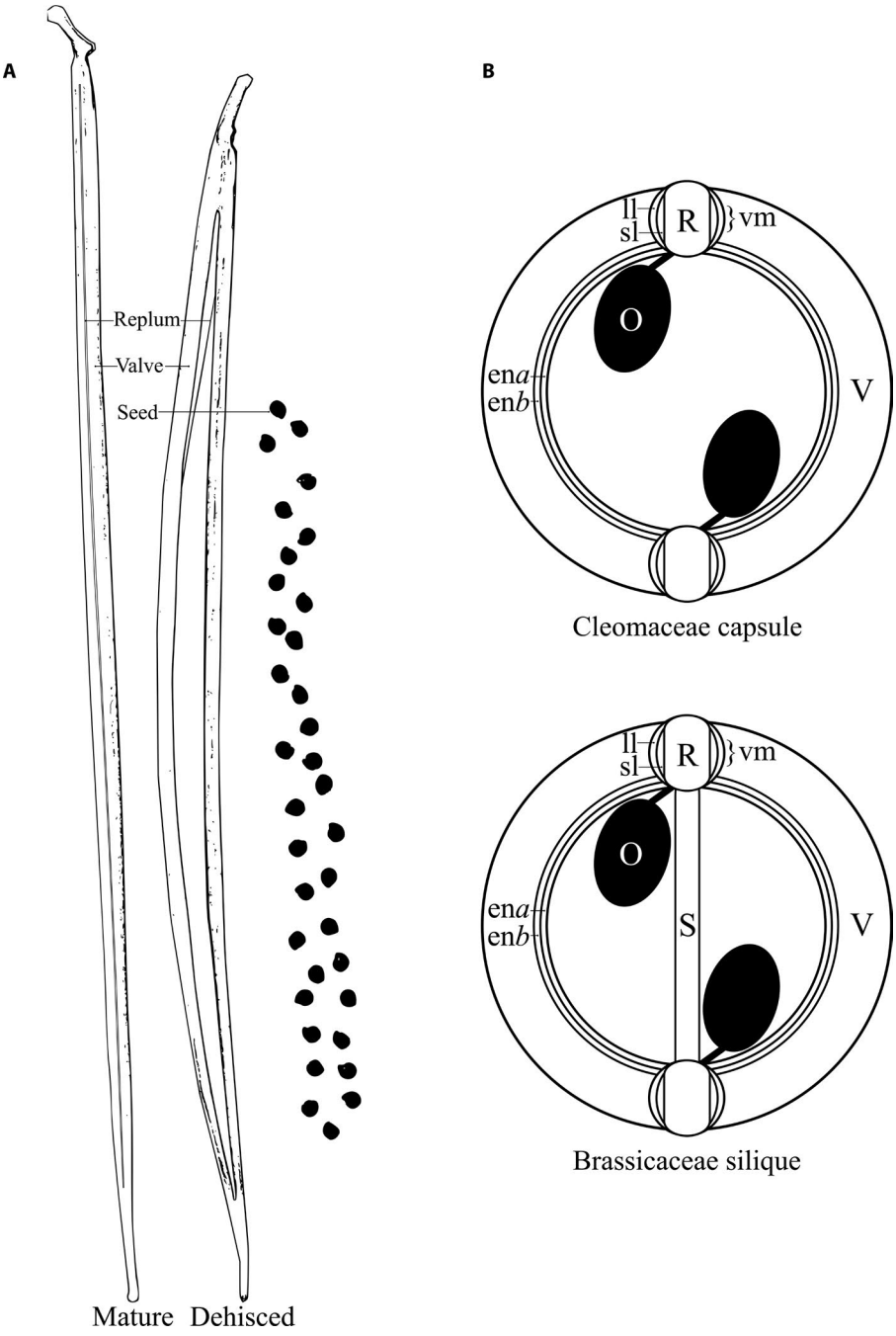

FIGURE 2. Line drawings of *Cleome violacea*. (A) *Cleome violacea* fruit at maturity and after dehiscence. (B) Diagram of Cleomaceae and Brassicaceae fruits in the transverse plane, showing the lignification layer (ll), separation layer (sl), valve margin (vm), replum (R), valve (V), endocarp layer (en*a*/*b*), ovary (O), and septum (S).

Resource (TAIR; https://www.arabidopsis.org) using their stock center (Arabidopsis Biological Resource Center [ABRC], Ohio State University, Columbus, Ohio, USA; https://abrc.osu.edu). The pTRV1 vector is required for viral movement (Ziegler-Graff et al., 1991), and the pTRV2 vector contains the gene of interest inserted into the multiple cloning site (MCS) (Ratcliff et al., 2001). Three endogenous constructs were also generated using *C. violacea* mRNA: pTRV2-*CvPDS*, pTRV2-*CvFUL*, and a pTRV2-*CvPDS*-*CvFUL* hybrid (Appendix S1).

RNA was extracted from *C. violacea* leaves, and separately from whole flowers, using a Concert Plant RNA Reagent Kit (Invitrogen, Carlsbad, California, USA), and was then treated with DNase I (Fermentas, Hanover, Maryland, USA) and enriched using an RNeasy Mini Kit (QIAGEN, Germantown, Maryland, USA). The mRNA was isolated using a Dynabeads mRNA Purification Kit (Invitrogen). The cDNA was synthesized using SuperScript III Reverse Transcriptase (Invitrogen), poly(T) primers, and random hexamer primers, following manufacturer instructions. *Arabidopsis thaliana PDS3* degenerate primers (Appendix S1) were used to amplify a 953-bp fragment from leaf cDNA. This fragment was then cloned into a TOPO-TA plasmid vector (Invitrogen) following the manufacturer instructions, and sequenced using BigDye Terminator sequencing (Applied Biosystems, Foster City, California, USA) with vector-specific primers M13F and M13R (Applied Biosystems). From that sequence, new primers were designed to amplify a 441-bp fragment with XbaI and BamHI restriction sites on the 5′ and 3′ fragment ends, respectively (Appendix S1). Alternatively, *CvFUL* primers with 5′ XbaI and 3′ BamHI restriction enzymes were designed using an unpublished transcriptome (Appendix S1); the primers amplify from the fifth exon to the eighth exon of the coding sequence, which avoids silencing other MADS-box genes with a conserved domain sequence. A 272-bp fragment of the *CvFUL* coding sequence was amplified using those primers and floral cDNA (Appendix S1). A *CvFUL*-*CvPDS* construct was also made using modified primers of *CvPDS* with a 5′ BamHI and 3′ XhoI restriction site. This modification enabled the ligation of a *CvPDS* construct to the 3′ end of *CvFUL* (Appendix S1). Restriction-modified fragments of *CvPDS*, *CvFUL*, and *CvFUL*-*CvPDS* were first cloned into TOPO-TA plasmid, and then excised and ligated into separately digested TRV2 vectors using XbaI, BamHI, and XhoI restriction enzymes and T4 DNA ligase (Promega Corporation, Fitchburg, Wisconsin, USA).

Viral constructs were verified for off-target silencing using siFi21 (Version 1.2.3-0008) (Lück et al., 2019). This software predicts off-targets of RNA interference (RNAi) by comparing user-defined sequences to a local database with Bowtie, a short-read aligner (Langmead et al., 2009; Langmead, 2010). Because Bowtie is purpose built for aligning to a reference, we used the *C. violacea* genome for tracking off-target silencing. One notable limitation is that Bowtie does not distinguish between introns and exons, thus any mRNA sequence that spans two exons may not be recognized. However, because the small interfering RNAs (siRNAs) tested are 21 bp in length, most targets will

still be identified. For clarification, the average exon length of the closely related *A. thaliana* is 236.8 bp (Koralewski and Krutovsky, 2011). Assuming *C. violacea* is similar, 21-bp siRNAs will produce many hits within each exon. We defined on-target sequences by using the BLAST (Altschul et al., 1990) function on https://genomevolution.org/coge. Coding sequences of *AtPDS* and *AtFUL* were matched using BLASTN against the *C. violacea* genome, and hits with the top *E*-values/bit-scores were defined as on-target. TRV2-*AtPDS*, TRV2-*CvPDS*, and TRV2-*CvFUL* were also aligned to the *C. violacea* genome as another way of verifying their similarity to *AtPDS* and *AtFUL*. The *C. violacea* genome is divided into scaffolds with sizes that range between 904 bp and 3.8 Mbp, so any sequences aligning to similar positions on the same scaffold are likely related.

TRV2 vectors were then cloned into One Shot TOP10 chemically competent *Escherichia coli* (Invitrogen) according to the manufacturer instructions. These *E. coli* were plated onto lysogeny broth (LB) agar plates containing 50 μg/mL kanamycin and grown overnight at 37°C. Colonies were screened via PCR with primers, 156F and 156R (Appendix S1), that span the TRV2 MCS (Gould and Kramer, 2007). Positively screened transformants were grown in LB media with the same antibiotics overnight at 37°C, and their plasmid constructs were purified using a QIAGEN Miniprep kit. Construct identity was confirmed using BigDye Terminator sequencing and 156F and 156R primers. All sequences were obtained with an ABI-3730 DNA Analyzer (Applied Biosystems) after being cleaned with a Performa DTR V3 96-well Short Plate Kit (Edge BioSystems, Gaithersburg, Maryland, USA). Nucleotide sequence of the *CvPDS* construct was deposited under the accession MW505002 in the National Center for Biotechnology Information (NCBI) GenBank, and a partial coding sequence of *CvFUL* is available under the accession MK584560.

Agrobacterium tumefaciens preparation and infiltration

Agrobacterium tumefaciens was prepared for DNA transformation as previously described (Weigel and Glazebrook, 2002). The following vectors were transformed into *A. tumefaciens* using calcium chloride heat-shock transformation: pTRV2-*AtPDS*, pTRV2-*CvPDS*, pTRV2-*CvFUL*, pTRV2-*CvPDS-CvFUL*, pTRV2-MCS, and pTRV1. For each, 100 ng of purified construct was combined with 250 μL of competent *A. tumefaciens*. Transformants were plated on LB media containing 50 μg/mL kanamycin, 50 μg/mL gentamycin, and 25 μg/mL rifampicin; all LB media used to grow *A. tumefaciens* contained these antibiotics. Transformants were then screened as before using 156F and 156R primers (Appendix S1), and glycerol stocks were made and stored at −80°C (1 : 1 ratio of 50% glycerol and overnight *A. tumefaciens* culture).

Vacuum infiltration was the chosen method for *C. violacea* because of its simplicity and efficiency compared with other methods (Wang et al., 2006; Becker and Lange, 2010). Alternative methods, such as agrodrench and booster inoculation (Ryu et al., 2004; Senthil-Kumar and Mysore, 2014), were briefly explored, but were abandoned due to low penetrance (data not shown). The first vacuum infiltration experiments were conducted to examine mortality and penetrance of plants at different developmental stages with heterologous and endogenous constructs. First, plants were categorized based on the number of true leaves: small with 0–3 true leaves, medium with 4–6 true leaves, and large with seven or more true leaves. To prepare for infiltration, *A. tumefaciens* containing each prepared vector was streaked onto LB agar with antibiotics and incubated for 72 h at room temperature. Individual colonies were used to inoculate 5 mL of LB with antibiotics, which were grown overnight at room temperature with constant shaking of 275 rpm to an OD600 of approximately 1.0. Sequential inoculations using the same media and conditions were then used to scale up growth to a final working volume of 500 mL. That is, 5-mL cultures were used to inoculate 50 mL of LB, which were used as starter cultures for 500 mL. Starter cultures one-tenth of the total volume produce sufficient growth in ~24 h. This process can be scaled up or down depending on the desired number of treated seedlings, and we recommend 500 mL for treatment groups with 50 to 100 seedlings. The final cultures contained: antibiotics, 1 mM MES buffer, and 0.02 mM acetosyringone. For each TRV2-containing *A. tumefaciens* culture, one pTRV2-containing *A. tumefaciens* culture must be grown because a 1 : 1 mixture is required for infiltration. Each culture was then aliquoted into 50-mL conical centrifuge tubes and centrifuged at 3200 *g* for 20 min at 4°C. The supernatant was decanted from each tube, and cells were resuspended in 20 mL of infiltration buffer (10 mM MES, 10 mM $MgCl_2$, and 0.2 mM acetosyringone). Resuspended colonies were recombined in a sterile beaker, and infiltration buffer was added to an OD600 of 2.0 ± 0.1. Colonies were then left at room temperature for a minimum of 4 h to acclimatize. It should be noted that it is also viable to leave cultures overnight if conditions are sterile.

The pTRV2 *A. tumefaciens* resuspensions were combined 1 : 1 with pTRV1 *A. tumefaciens* resuspensions. Silwet L-77 surfactant was added to each mixture at 100 μL/L. Groups of seedlings were extracted from the soil, rinsed in distilled water, and briefly air-dried before being submerged in the resuspensions and placed in a vacuum chamber. The vacuum chamber was evacuated for 10 sec, or until the mixture bubbled, and then the vacuum was turned off and seedlings were left for 2 min before pressure was quickly released. The resuspension mixtures were as follows: pTRV1 + pTRV2-*CvPDS*, pTRV1+ pTRV2-*AtPDS*, pTRV1 + pTRV2-*CvFUL*, pTRV1 + pTRV2-*CvFUL-CvPDS*, and pTRV1 + pTRV2-MCS as a negative control. Ten seedlings were infiltrated each time, and the same mixtures were reused for repeated infiltrations (i.e., 10 more seedlings up to 100 seedlings per 500 mL). Additionally, a group of seedlings were extracted from the soil, rinsed, and air-dried, and then replanted as an untreated control.

Phenotypic scoring varied depending on construct. Phenotypes for both *CvPDS*- and *AtPDS*-downregulated plants became apparent between three and four weeks post-inoculation. Plants treated with pTRV2-*CvPDS* and pTRV2-*AtPDS* had their leaves scored using visual approximation of bleaching and were binned into the following categories: pale (<50% of total bleaching), variegated (50–80%), and strong (>80%). Plants treated with pTRV2-*CvFUL* and pTRV2-*CvFUL-CvPDS* were scored approximately 30 days after vacuum infiltration. Phenotypes were initially binned into three categories based on the severity of fruit curling and the indentation of valve tissue around the ovules: (1) indentation only, (2) mild curling with indentation, and (3) heavy curling with indentation. These data were used to compare the effects of *CvFUL* silencing to *FUL* knockout in *A. thaliana* (Gu et al., 1998), although less severe phenotypes were expected because of incomplete mRNA silencing inherent to VIGS.

Leaf and fruit tissue from treated and control plants were excised, flash-frozen in liquid nitrogen, and stored at −80°C. Following described protocols (Patchell et al., 2011), scanning electron microscopy (SEM) was used to examine both untreated *C. violacea* and pTRV2-*CvFUL-CvPDS*-treated fruits. Leaf and fruit phenotypes

were imaged using a Nikon SMZ 1500 dissecting microscope (Nikon, Tokyo, Japan) with a QImaging Retiga 4000R camera (Teledyne DALSA, Waterloo, Ontario, Canada), and handheld digital Canon DS126181 camera (Canon, Tokyo, Japan). Images were standardized, scaled, color balanced, and assembled into figures using Inkscape version 0.92.5 (https://inkscape.org) and GIMP version 2.10.18 (https://www.gimp.org).

RT-qPCR expression analysis

RNA was extracted from approximately 100 mg of treated and control leaf and fruit tissue using an RNeasy Plant Mini Kit (ID:74904) (QIAGEN). The following amendments were made to their Quick-Start protocol: Step 1a, tissue was disrupted with a miniature pestle directly in a 1.5-mL Eppendorf tube. Step 1b was skipped. In Step 2, RLC buffer was used in lieu of RLT buffer for fruit tissue, and tubes were left to incubate at room temperature for 6 min with 1 min of vortexing at 2500 rpm. Step 6 was replaced with steps 4 and 5 from the QIAGEN Micro Kit Quick-Start Protocol to incorporate the column-based DNase I treatment. Step 10 was incubated for 5 min, and eluate was run through the same column twice. All steps with 15 sec centrifuge directions were increased to 30 sec due to centrifuge timer limitations. RNA was quantified and checked for integrity using the NanoDrop ND-1000 (version 3.1; Thermo Fisher Scientific, Waltham, Massachusetts, USA) and Bioanalyzer 2100 (version B.02.09.SI720; Agilent, Santa Clara, California, USA) from the Molecular Biology Service Unit, University of Alberta, Canada. The cDNA for each sample was generated as previously described using 1000 ng of RNA.

Quantitative reverse transcriptase PCR (RT-qPCR) was used to compare relative transcript levels between treated and untreated controls using the delta-delta Ct method. All experiments used *ACTIN* as a reference gene. Primers were designed using Primer Express 3.0 (Applied Biosystems), ensuring at least one primer was outside of the construct (Appendix S1). Primers were also tested for optimal efficiency using a dilution series. RT-qPCR was run using 10-μL reaction volumes containing 5.0 μL SYBR Green master mix (0.25× SYBR Green, 0.1× ROX, 0.3 units Platinum *Taq* Polymerase [Invitrogen], and 0.2 mM dNTPs), 2.5 μL of 3.4 μM forward and reverse primer, and 20 ng of cDNA. Assays were run using both the 384-well QuantStudio 6 Real-Time PCR System and the 7500 Fast Real-Time PCR System (both from Applied Biosystems). Three technical replicates per sample were analyzed with a minimum of three biological replicates (range of 3 to 5). One individual plant is equivalent to one biological replicate. VIGS-treated plants will often display varying phenotypes on one plant, and in such cases only one phenotype was used for RT-qPCR.

RESULTS

No off-target silencing was detected for endogenous pTRV2 constructs

The endogenous constructs had no off-target silencing and were on-target for our genes of interest. The coding sequence of *AtPDS* had top hits to scaffold 38 (650,987 bp), similar to both endogenous and heterologous constructs. The coding sequence of *AtFUL* had a top hit with scaffold 1565 (19,090 bp), similar to TRV2-*CvFUL*, which only had a single hit. No off-targets were found for TRV2-*CvPDS*, TRV2-*CvFUL*, or TRV2-*CvPDS*-*CvFUL*, and only minimal off-target silencing was detected for TRV2-*AtPDS* (Appendix S2). TRV2-*AtPDS* had 84 total and 36 efficient hits to scaffold 38. TRV2-*AtPDS* also had six off-target hits to scaffold 283 (212,661 bp), although none were efficient. The efficient hits are matched on a more stringent set of parameters and can be considered more representative of true off-targets (Lück et al., 2019). In summary, there were no major off-target sites for any of the constructs, and all constructs appear to target our genes of interest, *PDS* and *FUL*.

Agrobacterium tumefaciens–mediated pTRV2-*AtPDS* and pTRV2-*CvPDS* infection induces silencing of gene targets in *Cleome violacea*

An effective VIGS system entails low mortality and high penetrance of transient mutant phenotypes. We explored mortality and penetrance in *C. violacea* using binary vectors pTRV1 + pTRV2-*CvPDS* and pTRV1 + pTRV2-*AtPDS*. Initial experiments tested both heterologous (pTRV2-*AtPDS*) and endogenous (pTRV2-*CvPDS*) constructs to determine how susceptible *C. violacea* is to VIGS (Fig. 3). Treatment with pTRV2-*AtPDS* revealed that *C. violacea* was amenable to VIGS, as most surviving plants exhibited photobleaching (Table 1, Fig. 3A–E). Of the 198 plants treated with pTRV2-*AtPDS*, 119 survived, with roughly half displaying photobleaching. Relative to pTRV2-*AtPDS*, plants treated with pTRV2-*CvPDS* had the highest penetrance (81%) despite a lower survival rate (Table 1, Fig. 3F–J). The greatest penetrance (74%) was in medium plants (Table 1). That is, 37 of the 58 surviving plants that showed altered morphology were medium-sized seedlings (Table 1). Ultimately, medium plants were chosen for all subsequent experiments because of their stronger response to infiltration, i.e., stronger photobleaching. We also tested a species of Brassicaceae, *Erucaria erucarioides* Müll. Berol., with heterologous pTRV2-*AtPDS*, but no further experiments with *E. erucarioides* were completed due to low penetrance (Appendix S3). We mention these preliminary data to show that phylogenetic distance, and similarity of VIGS construct to the target gene, does not necessarily correlate with efficacy of VIGS (Appendix S4).

Follow-up experiments tested whether the observed phenotypes were due to downregulation of *CvPDS*. Here, we only used TRV2-*CvPDS* because it had the highest overall penetrance from earlier trials. The pTRV2-*CvPDS* treatment group had 36 of 86 surviving plants display photobleaching, most with strong photobleaching (Table 2). On average, we observed photobleaching from three to four weeks after inoculation, with the altered phenotypes lasting for several weeks. Leaves showing 50–80% and >80% photobleaching had significant downregulation of *CvPDS* relative to controls and treated plants with unaltered phenotype (Fig. 4A). Although we scored and phenotyped leaves with pale bleaching (1–50%) (Appendix S5A), they were not included in the RT-qPCR analysis because we are primarily interested in strong VIGS penetrance, i.e., our goal was to demonstrate that *CvPDS* is downregulated when we see obvious photobleaching. Leaves with complete photobleaching were also scored (Appendix S5A); however, they were binned with strong photobleaching (>80%) because of their infrequency. These results demonstrate that VIGS functions well in *C. violacea*, is experimentally replicable, and produces strong silencing with endogenous and heterologous constructs.

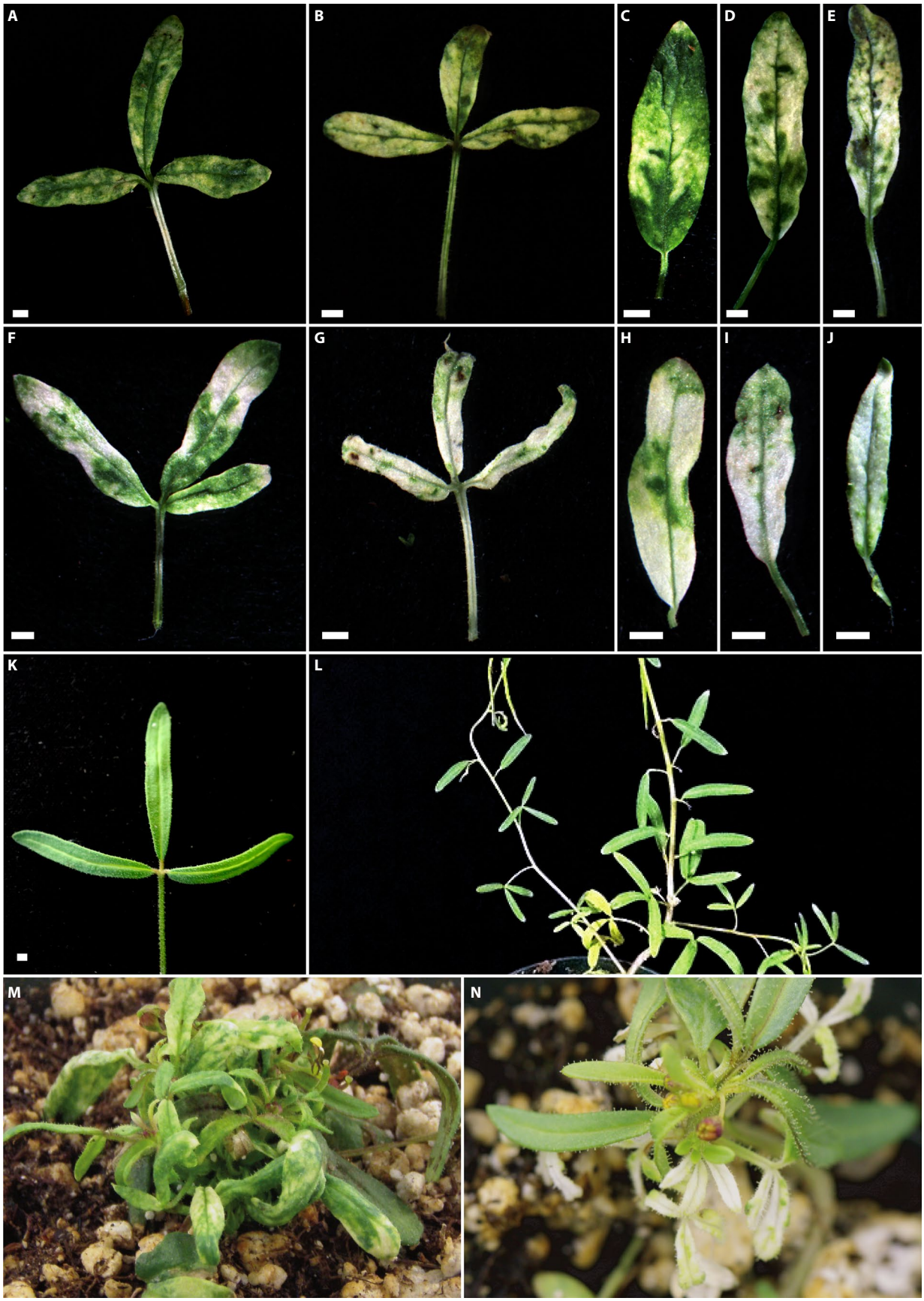

FIGURE 3. *Cleome violacea* subjected to virus-induced gene silencing (VIGS) using both heterologous and endogenous pTRV2-*CvPDS* constructs. (A, B) Leaves after silencing using *AtPDS* displaying pale (A) and variegated (B) photobleaching. (C–E) Leaflets silenced with *AtPDS* displaying pale (C) and variegated (D, E) photobleaching. (F, G) Leaves after treatment with *CvPDS* showing variegated (F) and strong (G) photobleaching. (H–J) Leaflets silenced with *CvPDS* displaying variegated (H) and strong (I, J) photobleaching. (K, L) Untreated *C. violacea* leaf (K) and whole plant (L). (M, N) Whole plant views of *C. violacea* treated with *AtPDS* (M) and *CvPDS* (N). Scale bar = 2 mm.

Agrobacterium-mediated pTRV2-*CvFUL* infection disrupts fruit morphology in *Cleome violacea*

Another factor in an effective VIGS system is the ability to study genes across developmental stages. As such, we investigated pTRV2-*CvFUL* treatment on the final stage of reproduction in flowering plants, fruit development. Fruits of *C. violacea* are elongate, bicarpellate capsules, which are characteristic for Cleomaceae. Like Brassicaceae, the fruits have valves, which are the portion of the ovary walls that separate at maturity (Fig. 2A). Also, like Brassicaceae, fruits of *C. violacea* have a prominent persistent placenta called the replum. The primary difference between Cleomaceae capsule fruits and Brassicaceae siliques is that Cleomaceae fruits lack the false septum separating the two locules (Fig. 2B) (Iltis et al., 2011). Like with *PDS*, initial experiments with pTRV2-*CvFUL-CvPDS* were completed to determine effectiveness in *C. violacea*. The *PDS* marker was used to facilitate phenotyping, as we were unsure of the silencing effects of *CvFUL* alone. Large seedlings were chosen for the initial experiments to account for developmental timing of fruiting. A range of altered fruit morphologies were observed four to six weeks post-inoculation. Of the 60 large seedlings treated (≥7 true leaves), there was a 95% survival rate, and 36% of survivors displayed some degree of curling and/or indentation (Table 1, Fig. 5A–D).

Later experiments used pTRV2-*CvFUL* alone, as initial experiments were relatively easy to score. Like with pTRV2-*CvFUL-CvPDS*, pTRV2-*CvFUL*-treated plants began displaying altered fruit morphologies by four to six weeks post-inoculation (Table 2, Fig. 5E–H). Most prominently, fruit curling and ovule indentation were observed, i.e., the valve was appressed around the developing seeds (Fig. 5E–H, Appendix S5H, I). In non-control treated plants of *C. violacea*, fruit length was decreased when fruit curling was moderate to heavy (≥90°); however, those with light curling (<90°) and/or indentation did not have a significant difference relative to fruits with non-altered phenotype (Appendix S6). Future studies with *CvFUL* knockouts would be more informative because variability of PTGS response is likely a major factor in fruit length with VIGS. For seedlings treated with pTRV2-*CvFUL*, 37 of the 85 surviving plants showed some altered phenotype, mostly mild curvature (Table 2). Incomplete and broad variability of *CvFUL* silencing made it difficult to accurately bin phenotypes by severity (Fig. 5E–H), despite initial efforts (Appendix S5B–E). Because our primary goal was to assess the general viability of *CvFUL* silencing using VIGS, and thus the potential for other fruit-patterning genes, we pooled data from all curled fruits for RT-qPCR regardless of severity. This way, ambiguities from incomplete silencing and unknown effects would be reduced while still demonstrating that *CvFUL* had been successfully downregulated. *CvFUL* was significantly downregulated relative to untreated plants, pTRV2-MCS-treated plants, and normal-phenotype treated plants (Fig. 4B). It should be noted that pTRV2-MCS had a greater than expected effect on fruit morphology (Appendix S5C, G); this is due to viral vector response and not downregulation of *CvFUL* (Fig. 4B). It seems likely that *C. violacea* fruits are more sensitive to tobacco rattle virus relative to other structures, which may account for the mild bulging in some fruits (Appendix S5G). It would be informative for future studies to observe the effects of viral response at varying concentrations of *A. tumefaciens* inoculation.

The curling, indentation, and shortening of fruits in pTRV2-*CvFUL-CvPDS*-treated plants are accompanied by differences in both cell size and shape in the valves and repla of those fruits (Fig. 6). Cells in the repla of pTRV2-*CvFUL-CvPDS*-treated plants are less elongated and less uniformly dispersed than their untreated counterparts (Fig. 6B, F). Furthermore, their ends are blunter and less tapered than in untreated plants. Cells in the valve regions also show marked differences between untreated and treated plants (Fig. 6C, D, G, H). Specifically, the smaller valve cells of pTRV2-*CvFUL*-treated plants are uneven and irregularly spaced (Fig. 6H). Smaller valve cells in untreated plants are more elongated, with even edges, and are somewhat regularly spaced (Fig. 6D). Both treated and untreated fruits have larger bulbous cells in their valve regions (Fig. 6C, G), although those from *CvFUL-CvPDS*-treated plants appear to be smaller, rounder, and less raised. Both untreated and treated fruits have glandular and multicellular trichomes, although they seem to be in greater number on treated fruits (Fig. 6C, G). The apparent increase seems likely to be a secondary effect of VIGS, as trichomes are known to be involved in pathogen response (Wang et al., 2021). Overall, these results demonstrate that silencing of *CvFUL* in *C. violacea* produces modified phenotypes in both valve and replum tissue.

DISCUSSION

VIGS is a well-established method for gene knockdown in angiosperms and has provided insight in determining the mechanisms

TABLE 1. Survival and penetrance data combined from multiple *Cleome violacea* virus-induced gene silencing trials. Mortality percentages were taken prior to 30 days post-inoculation. Plants were categorized based on the number of true leaves: small (s) with 0–3 true leaves, medium (m) with 4–6 true leaves, and large (l) with ≥7 true leaves.

	N				% Survival			% Penetrance (total)			% Penetrance (survivors)		
Treatment	**s**	**m**	**l**	**Total**	**s**	**m**	**l**	**s**	**m**	**l**	**s**	**m**	**L**
Untreated	23	30	18	71	87	80	94	NA	NA	NA	NA	NA	NA
pTRV2-MCS	49	85	21	155	10	38	86	NA	NA	NA	NA	NA	NA
pTRV2-*AtPDS*	51	68	79	198	18	78	72	61	57	37	22	74	51
pTRV2-*CvPDS*	25	121	77	223	0	21	43	0	14	22	0	81	52
pTRV2-*CvFUL-CvPDS*	NA	2	60	62	NA	50	95	NA	0	34	NA	0	36

Note: N = number of individuals sampled; NA = not applicable.

TABLE 2. Survival and penetrance data, representing two virus-induced gene silencing trials of medium plants (4–6 true leaves) of *Cleome violacea* grouped by treatment.

Treatment	*N*	% Survival	% Penetrance (total)	% Penetrance (survivors)
Untreated	50	86	NA	NA
Vacuum + surfactant	50	90	NA	NA
pTRV2-MCS	100	80	NA	NA
CvPDS	100	86		
0% bleached			51	44
<50% bleached			7	6
50–80% bleaching			8	7
>80% bleaching			34	29
CvFUL	100	85		
Indentation			8	9
Mild curvature			28	33
Moderate curvature			8	9
Heavy curvature			1	1

Note: N = number of individuals sampled; NA = not applicable.

underlying differences across diverse lineages such as Ranunculales, asterids, Caryophyllales, and rosids. It remains a powerful tool to address questions about organ identity, sex determination, induction of flowering, and compound leaf development (Hidalgo et al., 2012; Hsieh et al., 2013; Fujita et al., 2019). As such, the major goal of this study was to establish VIGS in Cleomaceae, which is garnering interest as a model family (Bayat et al., 2018). We established that *C. violacea* has high silencing efficiency and moderate mortality with VIGS treatment. Furthermore, *C. violacea* is amenable to treatment with readily available *Arabidopsis* constructs, which implies a potential to explore this method for additional members of Cleomaceae. Finally, we demonstrate that both leaves and fruits are susceptible to treatment, suggesting that other developmental stages and organs could also be studied with this system.

Arabidopsis thaliana constructs are valuable for assessing susceptibility to VIGS in Cleomaceae

Initial screens carried out on small, medium, and large seedlings with a heterologous *PDS* construct (pTRV2-*AtPDS*) were informative about overall susceptibility of *C. violacea* to VIGS (Table 1, Fig. 3A–E). Readily available heterologous constructs are a useful first pass for determining whether select species from Cleomaceae are amenable to VIGS. Survival and penetrance percentages were similar in *C. violacea* between both heterologous and endogenous (pTRV2-*CvPDS*) *PDS* constructs (Tables 1, 2). Overall, more plants survived after treatment with the *A. thaliana* construct than the endogenous construct, and both constructs had a similar percentage of photobleaching in medium plants. The increased mortality in pTRV2-*CvPDS*-treated plants was likely due to stronger photobleaching because photobleaching reduces efficiency of photosystem II (Wang et al., 2009). The use of endogenous constructs resulted in significant downregulation of *CvPDS* in *C. violacea* (Fig. 4A). Downregulation of *PDS* is also observed in *Nicotiana benthamiana* Domin using *PDS* constructs

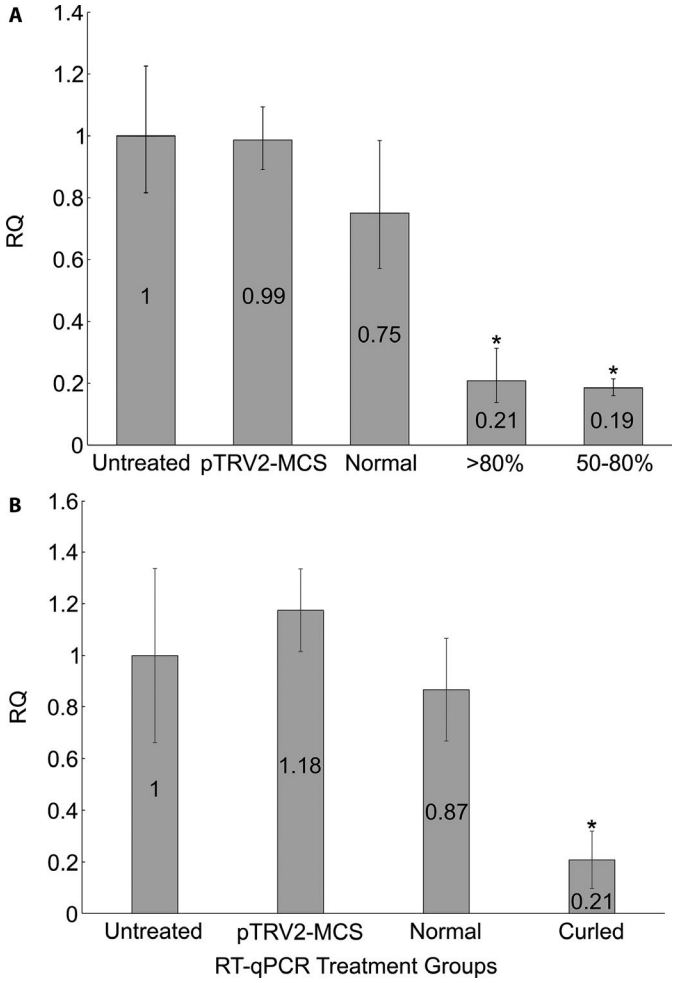

FIGURE 4. Relative quantification (RQ) vs. control of *PHYTOENE DESATURASE* (*CvPDS*)–silenced leaves (A) and *FRUITFULL* (*CvFUL*)–silenced fruits (B) from *Cleome violacea* after virus-induced gene silencing. (A) Untreated ($n = 4$), pTRV2-MCS ($n = 3$), normal phenotype ($n = 5$), >80% photobleaching ($n = 3$), and 50–80% photobleaching ($n = 3$). (B) Untreated ($n = 3$), pTRV2-MCS ($n = 3$), normal phenotype ($n = 3$), and curled ($n = 6$). Error bars indicate RQ maximum and minimum values calculated from standard error. *ACTIN* was used as an endogenous control. Statistical significance was determined using a Welch's *t*-test on delta CT means ($\alpha = 0.05$), indicated by an asterisk.

from other species of Solanaceae (Senthil-Kumar et al., 2007); even constructs from *Taxus baccata* (Pinophyta) were successfully used to downregulate *PDS* in *N. benthamiana* (Tafreshi et al., 2012). Close phylogenetic distance between *C. violacea* and *A. thaliana* was not indicative of higher susceptibility to VIGS, as another member of Brassicaceae had lower penetrance despite greater *PDS* sequence similarity (Appendices S4, S7). Different species displaying variable susceptibility to VIGS is unsurprising given that different cultivars of the same species, e.g., *Gerbera* (Asteraceae), also show different susceptibility to the same *PDS*

FIGURE 5. *Cleome violacea* subjected to virus-induced gene silencing using pTRV2-*CvFUL-CvPDS* (A–D) and pTRV2-*CvFUL* (E–H) constructs. (A–D) Fruits displaying photobleaching and atypical development after treatment with pTRV2-*CvPDS-CvFUL*. (E–H) Fruits displaying atypical development after treatment with pTRV2-*CvFUL*. pTRV2-*CvFUL-CvPDS*-treated *C. violacea* with normal development (I) and untreated fruit (J). Scale bar = 2 mm.

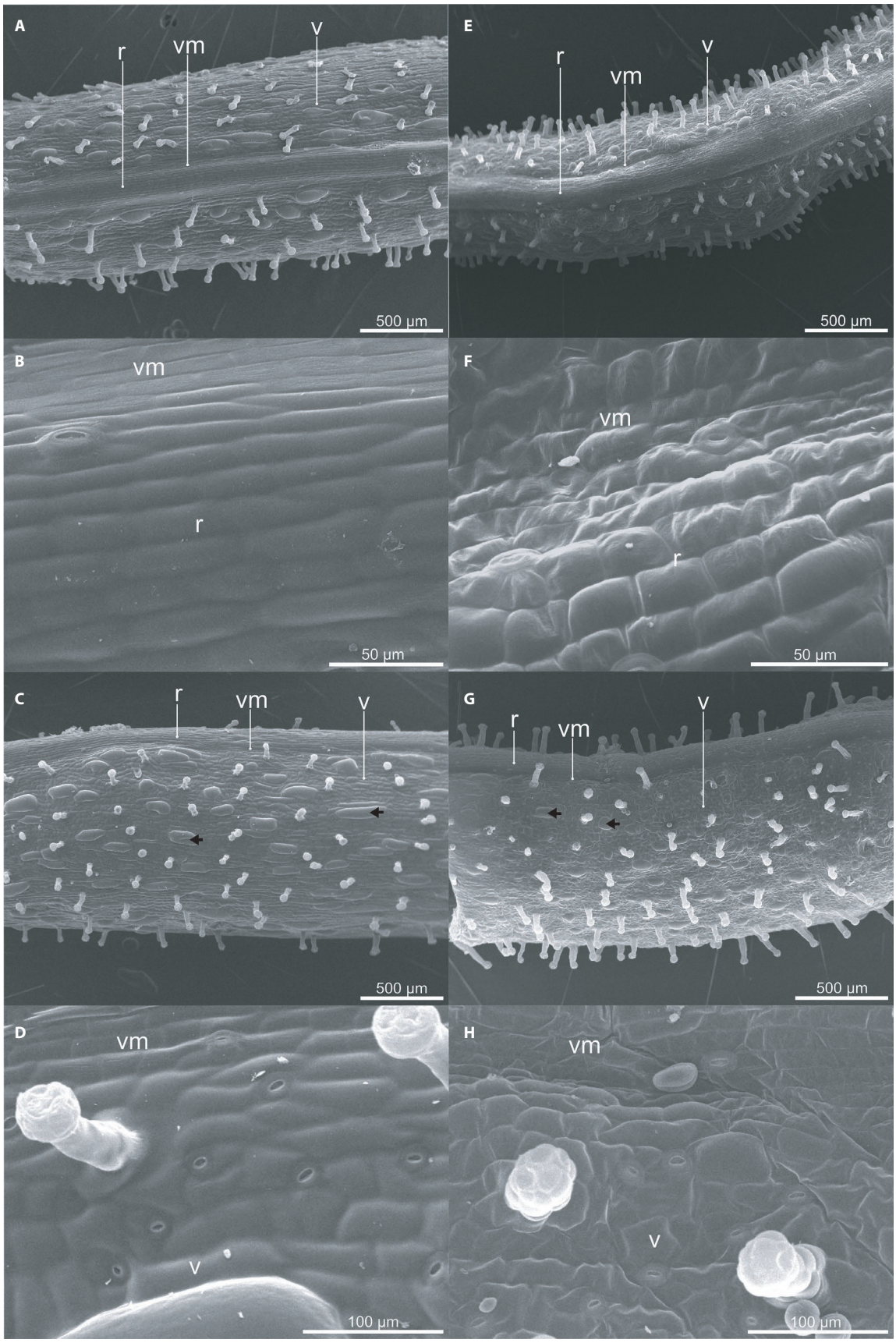

FIGURE 6. Scanning electron micrographs of untreated (A–D) and pTRV2-*CvFUL-CvPDS*–treated (E–H) *Cleome violacea* fruits. Medial view of untreated (A) and treated (E) fruit; medial view of untreated (B) and treated (F) replum and valve margin; lateral view of untreated (C) and treated (G) fruit; lateral view of untreated (D) and treated (H) valve and valve margin. Bulbous valve cells are indicated by black arrows. r = replum, v = valve, vm = valve margin.

vectors (Deng et al., 2012). That is, it appears that susceptibility to a specific vector, and to VIGS itself, is not necessarily predictable by phylogenetic distance.

There are many other factors in determining susceptibility, e.g., the type of viral vector, the length of the insert, and plant growth temperature. Although it varies by study, the effective lower limit for *PDS* silencing using TRV is as low as ~190 bp in *N. benthamiana* (Liu and Page, 2008), and even a size of 23 bp can produce silencing effects when using a potato virus vector (Thomas et al., 2001). Additionally, VIGS silencing appears to be more efficient at lower temperatures, and inhibited at high temperatures, in some species (e.g., *Lycopersicon esculentum* Mill. [tomato] [Fu et al., 2006], *Catharanthus roseus* (L.) G. Don [periwinkle] [Sung et al., 2014], and *Petunia ×hybrida* Hort. ex E. Vilm. [Broderick and Jones, 2014]); nonetheless, temperatures between 22–24°C function well for *C. violacea* and *A. thaliana* (Wang et al., 2006). Our data, in congruence with studies in *N. benthamiana*, strongly suggest that a construct sharing at least partial identity to the gene of interest is capable of knockdown, regardless of species origin. In summary, heterologous constructs are an informative first screen for VIGS in *C. violacea* and should be considered when exploring other members of Cleomaceae.

VIGS is a practical tool for studying fruit development in the Cleomaceae

Significant downregulation of the key fruit pattern gene *CvFUL* resulted in altered fruit morphology of *C. violacea* (Figs. 4B, 5). In preliminary treatments, *CvFUL* was downregulated in combination with a *CvPDS* marker (Table 1, Fig. 5A–D). We acknowledge the usefulness of marker genes for identifying difficult-to-spot mutant phenotypes and for quick identification when overall penetrance is low. However, there are limitations to marker genes. For example, in studies of floral symmetry, photobleaching would obscure pigmentation differences between adaxial and abaxial petals of *C. violacea* (Fig. 1). Additionally, there are potentially confounding effects of decreased plant vitality from photobleaching. For these reasons, and because *CvFUL*-silencing phenotypes are relatively easy to score, albeit difficult to bin, additional VIGS *CvFUL* treatments were completed without a marker (Fig. 5E–H).

FUL has a critical role in ensuring that the valve-margin genetic pathway is restricted to a thin layer of cells between the valve and replum in *A. thaliana* (Dinneny et al., 2005). Specifically, *FUL* is expressed in the valves and functions in positioning the valve margin in combination with *REPLUMLESS* (*REP*), which has a similar role in the replum. Given the similarities in overall fruit morphology between Brassicaceae and Cleomaceae (Fig. 2B), we predicted a conserved role in the genetic basis of fruit patterning via *FUL*. In *A. thaliana*, *ful-1* mutants have fruits with valve cells that have not properly developed and are much rounder than wild-type plants (Figs. 3, 7 from Gu et al., 1998). Mutant *ful A. thaliana* fruits and, to a lesser extent, other fruit-patterning mutants are shorter in length and have alterations in their valve cellular structure and uniformity (Fig. 4 from Liljegren et al., 2004). Like in *A. thaliana*, *CvFUL* influences the uniformity of cell expansion in the valve (Fig. 6D, H). Superficially, treated *C. violacea* fruits (Appendix S5D) appear more like *A. thaliana ful-1 35S::AGL8* rescue mutants (Fig. 7 from Gu et al., 1998), which are less stunted than *ful-1* mutants. Incomplete downregulation of *CvFUL* likely explains the somewhat normal fruit length observed during our trials.

Replum cells in fruits of *C. violacea* (Fig. 6F) are irregularly shaped in *CvFUL-CvPDS*-silenced fruits, a phenotype that is also observed in fruits of *ful-1 A. thaliana* mutants (Fig. 3E from Gu et al., 1998). We propose that the alteration in replum growth is likely due to shearing forces from the offset growth of valve tissue on either side, which is likely due to incomplete silencing of *CvFUL*. When *FUL* is downregulated, it prevents the formation of a dehiscence zone between the replum and the valve (reviewed in Ferrándiz and Fourquin, 2014). Thus, both sides of the valve variably push and pull on the replum, and because it cannot separate at the dehiscence zone, it warps the replum and causes fruit curling. A complete knockout of *CvFUL* should not curl because the replum valve boundary would be disrupted evenly along the length of the fruit, i.e., cells in the valves would exert even pressure on the replum. Altogether, these data exhibit how VIGS can be used to target late developmental stages prior to the initiation of those stages.

Cleomaceae is quickly emerging as a model family to address a range of evolutionary and developmental questions (Bayat et al., 2018). Additional functional tools are invaluable for examining the morphological novelties present in the family. We have demonstrated that mild modifications to established VIGS protocols (Gould and Kramer, 2007; Kramer et al., 2007) are sufficient for high penetrance of *PDS* and *FUL* mutant phenotypes in *C. violacea* (Tables 1, 2). We propose that use of *A. thaliana* constructs is a viable first step in future investigations of additional species in the family because of the effectiveness of pTRV2-*AtPDS* constructs in this study. Furthermore, the published draft genome of *C. violacea* makes this species a prime candidate for further research on a range of traits.

ACKNOWLEDGMENTS

The authors would like to thank the Natural Sciences and Engineering Research Council of Canada (NSERC; grant no. RGPIN-2014-04705) for funding.

AUTHOR CONTRIBUTIONS

P.M., M.H.D., J.C.H., and S.C. contributed to conception and design of the project. S.C., M.H.D., P.M., and A.R. contributed to data collection and analysis. S.C. and J.C.H. contributed to drafting and revising of the manuscript. All authors provided feedback on drafts and gave consent to publish the material.

DATA AVAILABILITY

The *CvPDS* construct sequence (accession no. MW505002) is available at the National Center for Biotechnology Information. Phenotyping and RT-qPCR raw data are available upon request.

SUPPORTING INFORMATION

Additional Supporting Information may be found online in the supporting information tab for this article.

APPENDIX S1. List of primers used for construct design and RT-qPCR in this study. Brackets indicate restriction sites for incorporation into the pTRV2 vector. Extra base pairs upstream of restriction sites are to improve digestion efficiency. EcoRI (G^AATTC), XbaI (T^CTAGA), BamHI (G^GATCC), and XhoI (C^TCGAG).

APPENDIX S2. SiFi21 results for pTRV2 constructs used in this study: (A) pTRV2-*CvFUL*, (B) pTRV2-*CvPDS*, (C) pTRV2-*CvFUL-CvPDS*, (D) pTRV2-*AtPDS*. Results are compared to the draft genome of *Cleome violacea* (https://genomevolution.org/coge; accession no. 23822) and organized by scaffolds.

APPENDIX S3. Hits to the *Cleome violacea* genome (https://genomevolution.org/coge; accession no. 23822) using *Arabidopsis thaliana* coding sequences of *FUL* and *PDS*, TRV2-*ATPDS*, TRV2-*CvPDS*, and TRV2-*CvFUL* constructs. Default parameters were used for CoGe BLASTN.

APPENDIX S4. Percent identity of the pTRV2-*AtPDS* construct relative to *PDS* from *Arabidopsis thaliana*, *Erucaria erucarioides*, and *Cleome violacea* (A). Graph of the alignment using Geneious alignment software with 93% similarity cost matrix and default settings (B).

APPENDIX S5. (A) *Cleome violacea* leaflets, taken from whole leaves with identical phenotypes, after treatment with pTRV2-*CvPDS*. From left to right: untreated, pale bleaching (0–50%); variegated bleaching (50–80%); strong bleaching (>80%); and complete bleaching. Scale bar = 2 mm. (B–I) *Cleome violacea* fruits after treatment with TRV2-*CvFUL*: untreated control (B, F), pTRV2-MCS (C, G), mild curvature with indentation (D, H), moderate curvature with indentation (E, I). r = replum, v = valve; vm = valve margin; arrows indicate indentation. Scale bars = 0.5 cm (B–E) and 500 μm (F–I).

APPENDIX S6. Length of *Cleome violacea* fruits treated with pTRV2-*CvFUL*. Normal phenotype (n = 24), indentation (n = 8), mild and moderate curvature with indentation (n = 5). Significance was determined using Welch's t-test (α = 0.01), indicated by an asterisk.

APPENDIX S7. Survival and penetrance data combined from multiple *Erucaria erucarioides* virus-induced gene silencing trials. Mortality percentages were taken prior to 30 days post-inoculation. Plants were categorized based on the number of true leaves: small (s) with 0–3 true leaves, medium (m) with 4–6 true leaves, and large (l) with ≥7 true leaves.

LITERATURE CITED

Altschul, S. F., W. Gish, W. Miller, E. W. Myers, and D. J. Lipman. 1990. Basic local alignment search tool. *Journal of Molecular Biology* 215: 403–413.

Barker, M. S., H. Vogel, and M. E. Schranz. 2009. Paleopolyploidy in the Brassicales: Analyses of the *Cleome* transcriptome elucidate the history of genome duplications in *Arabidopsis* and other Brassicales. *Genome Biology and Evolution* 1: 391–399.

Baulcombe, D. C. 1999. Fast forward genetics based on virus-induced gene silencing. *Current Opinion in Plant Biology* 2: 109–113.

Bayat, S., M. E. Schranz, E. H. Roalson, and J. C. Hall. 2018. Trends in plant science lessons from Cleomaceae, the little sister of crucifers. *Trends in Plant Science* 23: 808–821.

Becker, A. 2013. Virus-induced gene silencing. Humana Press, New York, New York, USA.

Becker, A., and M. Lange. 2010. VIGS: Genomics goes functional. *Trends in Plant Science* 15: 1–4.

Bhide, A., S. Schliesky, M. Reich, A. P. M. Weber, and A. Becker. 2014. Analysis of the floral transcriptome of *Tarenaya hassleriana* (Cleomaceae), a member of the sister group to the Brassicaceae: Towards understanding the base of morphological diversity in Brassicales. *BMC Genomics* 15: 140.

Bräutigam, A., K. Kajala, J. Wullenweber, M. Sommer, D. Gagneul, K. L. Weber, K. M. Carr, et al. 2011a. An mRNA blueprint for C_4 photosynthesis derived from comparative transcriptomics of closely related C_3 and C_4 species. *Plant Physiology* 155: 142–156.

Bräutigam, A., T. Mullick, S. Schliesky, and A. P. M. Weber. 2011b. Critical assessment of assembly strategies for non-model species mRNA-Seq data and application of next-generation sequencing to the comparison of C_3 and C_4 species. *Journal of Experimental Botany* 62: 3093–3102.

Broderick, S. R., and M. L. Jones. 2014. An optimized protocol to increase virus-induced gene silencing efficiency and minimize viral symptoms in petunia. *Plant Molecular Biology Reporter* 32: 219–233.

Burch-Smith, T. M., J. C. Anderson, G. B. Martin, and S. P. Dinesh-Kumar. 2004. Applications and advantages of virus-induced gene silencing for gene function studies in plants. *Plant Journal* 39: 734–746.

Burch-Smith, T. M., M. Schiff, Y. Liu, and S. P. Dinesh-Kumar. 2006. Efficient virus-induced gene silencing in Arabidopsis. *Plant Physiology* 142: 21–27.

Cane, J. H. 2008. Breeding biologies, seed production and species-rich bee guilds of *Cleome lutea* and *Cleome serrulata* (Cleomaceae). *Plant Species Biology* 23: 152–158.

Cheng, S., E. van den Bergh, P. Zeng, X. Zhong, J. Xu, X. Liu, J. Hofberger, et al. 2013. The *Tarenaya hassleriana* genome provides insight into reproductive trait and genome evolution of crucifers. *Plant Cell* 25: 2813–2830.

Deng, X., P. Elomaa, C. X. Nguyen, T. Hytönen, J. P. T. Valkonen, and T. H. Teeri. 2012. Virus-induced gene silencing for Asteraceae: A reverse genetics approach for functional genomics in *Gerbera hybrida*. *Plant Biotechnology Journal* 10: 970–978.

Di Stilio, V. S., R. A. Kumar, A. M. Oddone, T. R. Tolkin, P. Salles, and K. McCarty. 2010. Virus-induced gene silencing as a tool for comparative functional studies in *Thalictrum*. *PLoS ONE* 5: e12064.

Dinneny, J. R., D. Weigel, and M. F. Yanofsky. 2005. A genetic framework for fruit patterning in *Arabidopsis thaliana*. *Development* 132: 4687–4696.

Eldridge, T., Ł. Łangowski, N. Stacey, F. Jantzen, L. Moubayidin, A. Sicard, P. Southam, et al. 2016. Fruit shape diversity in the Brassicaceae is generated by varying patterns of anisotropy. *Development* 143: 3394–3406.

Endress, P. 2016. Evolution and floral diversity: The phylogenetic surroundings of *Arabidopsis* and *Antirrhinum*. *International Journal of Plant Sciences* 153: 106–122.

Ferrándiz, C., S. J. Liljegren, and M. F. Yanofsky. 2000a. Negative regulation of the *SHATTERPROOF* genes by *FRUITFULL* during Arabidopsis fruit development. *Science* 289: 436–438.

Ferrándiz, C., Q. Gu, R. Martienssen, and M. F. Yanofsky. 2000b. Redundant regulation of meristem identity and plant architecture by *FRUITFULL*, *APETALA1* and *CAULIFLOWER*. *Development* 127: 725–734.

Ferrándiz, C., and C. Fourquin. 2014. Role of the *FUL-SHP* network in the evolution of fruit morphology and function. *Journal of Experimental Botany* 65: 4505–4513.

Fu, D. Q., B. Z. Zhu, H. L. Zhu, H. X. Zhang, Y. H. Xie, W. B. Jiang, X. D. Zhao, and Y. B. Luo. 2006. Enhancement of virus-induced gene silencing in tomato by low temperature and low humidity. *Molecules & Cells* 21: 153–160.

Fujita, N., Y. Kazama, N. Yamagishi, K. Watanabe, S. Ando, H. Tsuji, S. Kawano, et al. 2019. Development of the VIGS system in the dioecious plant *Silene latifolia*. *International Journal of Molecular Sciences* 20: 1031.

Gould, B., and E. M. Kramer. 2007. Virus-induced gene silencing as a tool for functional analyses in the emerging model plant *Aquilegia* (columbine, Ranunculaceae). *Plant Methods* 3: 6.

Gu, Q., C. Ferrandiz, M. F. Yanofsky, and R. Martienssen. 1998. The *FRUITFULL* MADS-box gene mediates cell differentiation during Arabidopsis fruit development. *Development* 125: 1509–1517.

Hidalgo, O., C. Bartholmes, and S. Gleissberg. 2012. Virus-induced gene silencing (VIGS) in *Cysticapnos vesicaria*, a zygomorphic-flowered Papaveraceae (Ranunculales, basal eudicots). *Annals of Botany* 109: 911–920.

Higuera-Díaz, M., J. S. Manson, and J. C. Hall. 2015. Pollination biology of *Cleomella serrulata* and *Polanisia dodecandra* in a protected natural prairie in southern Alberta, Canada. *Botany* 93: 745–757.

Hsieh, M. H., H. C. Lu, Z. J. Pan, H. H. Yeh, S. S. Wang, W. H. Chen, and H. H. Chen. 2013. Optimizing virus-induced gene silencing efficiency with *Cymbidium* mosaic virus in *Phalaenopsis* flower. *Plant Science* 201: 25–41.

Iltis, H. H., J. C. Hall, T. S. Cochrane, and K. J. Systma. 2011. Studies in the Cleomaceae I. On the separate recognition of Capparaceae, Cleomaceae, and Brassicaceae. *Annals of the Missouri Botanical Garden* 98: 28–36.

Koralewski, T. E., and K. V. Krutovsky. 2011. Evolution of exon-intron structure and alternative splicing. *PLoS ONE* 6: e18055.

Koteyeva, N. K., E. V. Voznesenskaya, E. H. Roalson, and G. E. Edwards. 2011. Diversity in forms of C_4 in the genus *Cleome* (Cleomaceae). *Annals of Botany* 107: 269–283.

Koteyeva, N. K., E. V. Voznesenskaya, A. B. Cousins, and G. E. Edwards. 2014. Differentiation of C_4 photosynthesis along a leaf developmental gradient in two *Cleome* species having different forms of Kranz anatomy. *Journal of Experimental Botany* 65: 3525–3541.

Kramer, E. M., L. Holappa, B. Gould, M. A. Jaramillo, D. Setnikov, and P. M. Santiago. 2007. Elaboration of B gene function to include the identity of novel floral organs in the lower eudicot *Aquilegia*. *Plant Cell* 19: 750–766.

Külahoglu, C., A. K. Denton, M. Sommer, J. Mass, S. Schliesky, T. J. Wrobel, B. Berckmans, et al. 2014. Comparative transcriptome atlases reveal altered gene expression modules between two Cleomaceae C_3 and C_4 plant species. *Plant Cell* 26: 3243–3260.

Langmead, B. 2010. Aligning short sequencing reads with Bowtie. *Current Protocols in Bioinformatics* 32. https://doi.org/10.1002/0471250953.bi1107s32.

Langmead, B., C. Trapnell, M. Pop, and S. L. Salzberg. 2009. Ultrafast and memory-efficient alignment of short DNA sequences to the human genome. *Genome Biology* 10: R25.

Liljegren, S. J., A. H. K. Roeder, S. A. Kempin, K. Gremski, L. Østergaard, S. Guimil, D. K. Reyes, and M. F. Yanofsky. 2004. Control of fruit patterning in Arabidopsis by *INDEHISCENT*. *Cell* 116: 843–853.

Liu, E., and J. E. Page. 2008. Optimized cDNA libraries for virus-induced gene silencing (VIGS) using Tobacco Rattle virus. *Plant Methods* 4: 5.

Lück, S., T. Kreszies, M. Strickert, P. Schweizer, M. Kuhlmann, and D. Douchkov. 2019. siRNA-Finder (si-Fi) software for RNAi-target design and off-target prediction. *Frontiers in Plant Science* 10. https://doi.org/10.3389/fpls.2019.01023.

Mabry, M., J. Brose, P. Blischak, B. Sutherland, W. Dismukes, C. Bottoms, P. Edger, et al. 2020. Phylogeny and multiple independent whole-genome duplication events in the Brassicales. *American Journal of Botany* 107: 1148–1164.

Marshall, D. M., R. Muhaidat, N. J. Brown, Z. Liu, S. Stanley, H. Griffiths, R. F. Sage, and J. M. Hibberd. 2007. *Cleome*, a genus closely related to Arabidopsis, contains species spanning a developmental progression from C_3 to C_4 photosynthesis. *Plant Journal* 51: 886–896.

Newell, C. A., N. J. Brown, Z. Liu, A. Pflug, U. Gowik, P. Westhoff, and J. M. Hibberd. 2010. *Agrobacterium tumefaciens*-mediated transformation of *Cleome gynandra* L., a C_4 dicotyledon that is closely related to *Arabidopsis thaliana*. *Journal of Experimental Botany* 61: 1311–1319.

Nozzolillo, C., V. T. Amiguet, A. C. Bily, C. S. Harris, A. Saleem, Ø. M. Andersen, and M. Jordheim. 2010. Novel aspects of the flowers and floral pigmentation of two *Cleome* species (Cleomaceae), *C. hassleriana* and *C. serrulata*. *Biochemical Systematics and Ecology* 38: 361–369.

Patchell, M. J., M. C. Bolton, P. Mankowski, and J. C. Hall. 2011. Comparative floral development in Cleomaceae reveals two distinct pathways leading to monosymmetry. *International Journal of Plant Sciences* 172: 352–365.

Patchell, M. J., E. H. Roalson, and J. C. Hall. 2014. Resolved phylogeny of Cleomaceae based on all three genomes. *Taxon* 63: 315–328.

Ratcliff, F., A. Montserrat Martin-Hernandez, and D. C. Baulcombe. 2001. Tobacco Rattle virus as a vector for analysis of gene function by silencing. *Plant Journal* 25: 237–245.

Ruiz, M. T., O. Voinnet, and D. C. Baulcombe. 1998. Initiation and maintenance of virus-induced gene silencing. *Plant Cell* 10: 937–946.

Ryu, C. M., A. Anand, L. Kang, and K. S. Mysore. 2004. Agrodrench: A novel and effective agroinoculation method for virus-induced gene silencing in roots and diverse Solanaceous species. *Plant Journal* 40: 322–331.

Schranz, M. E., and T. Mitchell-Olds. 2006. Independent ancient polyploidy events in the sister families Brassicaceae and Cleomaceae. *Plant Cell* 18: 1152–1165.

Senthil-Kumar, M., R. Hema, A. Anand, L. Kang, M. Udayakumar, and K. S. Mysore. 2007. A systematic study to determine the extent of gene silencing in *Nicotiana benthamiana* and other Solanaceae species when heterologous gene sequences are used for virus-induced gene silencing. *New Phytologist* 176: 782–791.

Senthil-Kumar, M., and K. S. Mysore. 2014. Tobacco Rattle virus-based virus-induced gene silencing in *Nicotiana benthamiana*. *Nature Protocols* 9: 1549–1562.

Sung, Y. C., C. P. Lin, and J. C. Chen. 2014. Optimization of virus-induced gene silencing in *Catharanthus roseus*. *Plant Pathology* 63: 1159–1167.

Tafreshi, S. A. H., M. Shariati, M. R. Mofid, M. K. Nekui, and A. Esmaeili. 2012. Heterologous virus-induced gene silencing as a promising approach in plant functional genomics. *Molecular Biology Reports* 39: 2169–2178.

Thomas, C. L., L. Jones, D. C. Baulcombe, and A. J. Maule. 2001. Size constraints for targeting post-transcriptional gene silencing and for RNA-directed methylation in *Nicotiana benthamiana* using a potato virus X vector. *Plant Journal* 25: 417–425.

Tsai, Y. T., P. Y. Chen, and K. Y. To. 2012. Plant regeneration and stable transformation in the floricultural plant *Cleome spinosa*, a C_3 plant closely related to the C_4 plant *C. gynandra*. *Plant Cell Reports* 31: 1189–1198.

van den Bergh, E., J. A. Hofberger, and M. E. Schranz. 2016. Flower power and the mustard bomb: Comparative analysis of gene and genome duplications in glucosinolate biosynthetic pathway evolution in Cleomaceae and Brassicaceae. *American Journal of Botany* 103: 1212–1222.

Velasquez, A., S. Chakravarthy, and G. B. Martin. 2009. Virus-induced gene silencing (VIGS) in *Nicotiana benthamiana* and tomato. *Journal of Visualized Experiments* 28: e1292.

Voznesenskaya, E. V., N. K. Koteyeva, S. D. X. Chuong, A. N. Ivanova, J. Barroca, L. A. Craven, and G. E. Edwards. 2007. Physiological, anatomical and biochemical characterisation of photosynthetic types in genus *Cleome* (Cleomaceae). *Functional Plant Biology* 34: 247–267.

Wang, C., X. Cai, X. Wang, and Z. Zheng. 2006. Optimisation of Tobacco Rattle virus-induced gene silencing in Arabidopsis. *Functional Plant Biology* 33: 347–355.

Wang, M., G. Wang, J. Ji, and J. Wang. 2009. The effect of *pds* gene silencing on chloroplast pigment composition, thylakoid membrane structure and photosynthesis efficiency in tobacco plants. *Plant Science* 177: 222–226.

Wang, X., C. Shen, P. Meng, G. Tan, and L. Lv. 2021. Analysis and review of trichomes in plants. *BMC Plant Biology* 21: 70.

Wege, S., A. Scholz, S. Gleissberg, and A. Becker. 2007. Highly efficient virus-induced gene silencing (VIGS) in California poppy (*Eschscholzia californica*): An evaluation of VIGS as a strategy to obtain functional data from non-model plants. *Annals of Botany* 100: 641–649.

Weigel, D., and J. Glazebrook. 2002. Arabidopsis: A laboratory manual. Cold Spring Harbor Laboratory Press, Cold Spring Harbor, New York, USA.

Williams, B. P., S. J. Burgess, I. Reyna-Llorens, J. Knerova, S. Aubry, S. Stanley, and J. M. Hibberd. 2015. An untranslated *cis*-element regulates the accumulation of multiple C_4 enzymes in *Gynandropsis gynandra* mesophyll cells. *Plant Cell* 28: 454–465.

Ziegler-Graff, V., P. J. Guildford, and D. C. Baulcombe. 1991. Tobacco Rattle virus RNA-1 29K gene product potentiates viral movement and also affects symptom induction in tobacco. *Virology* 182: 145–155.

